MAY 14 1923

Volume 7 Number 5

Journal of the Optical Society of America and Review of Scientific Instruments

EDITOR-IN-CHIEF: PAUL D. FOOTE
BUREAU OF STANDARDS, WASHINGTON, D.C.

ASSISTANT EDITOR-IN-CHIEF AND BUSINESS MANAGER: F. K. RICHTMYER
CORNELL UNIVERSITY, ITHACA, N. Y.

CONSULTING BUSINESS MANAGER, M. E. LEEDS, Philadelphia, Pa.

Associate Editors:

Term Ending Dec. 31, 1927	Term Ending Dec. 31, 1925	Term Ending Dec. 31, 1923
H. D. CURTIS	G. K. BURGESS	W. T. BOVIE
E. P. HYDE	K. T. COMPTON	H. G. GALE
PAUL E. KLOPSTEG	L. R. INGERSOLL	HERBERT E. IVES
L. SILBERSTEIN	C. E. K. MEES	W. B. LANCASTER
L. T. TROLAND	C. E. MENDENHALL	P. G. NUTTING
F. E. WRIGHT	D. C. MILLER	J. P. C. SOUTHALL

MAY, 1923

A Chart of the Flicker Photometer 363
HERBERT E. IVES

Geometric Progression in Optically Prepared Standards 375
ARTHUR P. HARRISON

INSTRUMENT SECTION

A Device for Logarithmic and Semi-logarithmic Plotting and Finding Powers and Exponentials 377
R. A. CASTLEMAN, JR.

A Projection Electroscope for Measurements in Radioactivity 385
HOWARD M. ELSEY

A Precise Method of Measuring Small Emfs, and the Change in Thermoelectric Power of Tin at the Melting Point 389
T. R. HARRISON and PAUL D. FOOTE

The Design of Large Incandescent Lamps 399
P. G. NUTTING

A Projection Ammeter-Voltmeter 403
HOWARD M. ELSEY

A Method of Increasing the Dispersion of a Constant Deviation Spectroscope 405
J. F. T. YOUNG

Notes 373, 374, 383, 384, 388

Index to Advertisers XXXV

Published Monthly by the
OPTICAL SOCIETY OF AMERICA

OFFICE OF PUBLICATION:
GEORGE BANTA PUBLISHING COMPANY
MENASHA, WISCONSIN

Entered as second-class matter May 31, 1921 at the postoffice at Menasha, Wis., under the act of March 3, 1879.

Journal
of the
Optical Society of America
and
Review of Scientific Instruments

Published monthly beginning May 1922.
Annual Subscription $5.00

The JOURNAL of the Optical Society of America was first published in January 1917. Four separate issues appeared in 1917, and two issues in 1919. During the years 1920 (Vol. IV) and 1921 (Vol. V) the JOURNAL was published bi-monthly. Copies of back numbers may be secured from the Business Manager for $1.00 each. The total charge for all numbers from Vol. I to Vol. V, 1921 inclusive, is $16.00. Only a small stock of the earlier issues remains. The six numbers comprising Vols. I to III will not be sold except in complete sets with Vol. IV and V.

By cooperation with the Association of Scientific Apparatus Makers of the United States of America the scope of the JOURNAL was enlarged beginning January 1922. As indicated by the present title the JOURNAL now publishes original papers on instruments of every description as well as papers on experimental and applied optics. The new JOURNAL is published monthly beginning May 1922, making 10 issues for 1922.

Annual Subscription $5.00 dating from January of the current year. Single copies $0.60. Remittances for subscriptions and back numbers should be made to "F. K. Ritchtmyer, Manager," Cornell University, Ithaca, N. Y.

All correspondence on the following subjects must be made with the Business Manager: (1) Application for, and checks in payment of annual subscriptions other than those of members of the Optical Society; (2) Change in mailing address; (3) Missing numbers: these will be replaced free of charge only when notification is made within 30 days from date of the immediately succeeding issue; (4) All advertising accounts and applications for space and rates.

THE OPTICAL SOCIETY OF AMERICA

President—L. T. TROLAND,
Harvard University,
Cambridge, Mass.

Vice-President—H. E. IVES,
Western Electric Co.,
New York, N. Y.

Secretary—IRWIN G. PRIEST,
Bureau of Standards,
Washington, D. C.

Treasurer—ADOLPH LOMB,
Rochester, New York.

The Council consists of the above officers, the Editor-in-Chief and the Assistant Editor-in-Chief and Business Manager of the JOURNAL, the past President, James P. C. Southall, Columbia University, and the following elected members: Adelbert Ames, Dartmouth College, H. G. Gale, University of Chicago, Ernest Merritt, Cornell University and W. E. Forsythe, Nela Research Laboratories.

The object of the Optical Society of America is to serve the interests of all who are engaged in any branch of optics from fundamental research to the manufacture of optical goods.

The Constitution provides that anyone who has contributed materially to the advancement of optics shall be eligible to regular membership in the Society with the privilege of voting and holding office. Any individual or corporation interested in optics is eligible to associate membership. Annual dues including subscription to the JOURNAL are five dollars for individual membership and fifty dollars for corporation membership. Further information may be obtained from the Secretary.

Journal
of the
Optical Society of America
and
Review of Scientific Instruments

Vol. 7 MAY, 1923 Number 5

A CHART OF THE FLICKER PHOTOMETER

By Herbert E. Ives

Introduction

In various investigations of the phenomena of critical frequency and of the flicker photometer the writer has obtained a considerable body of experimental data. Part of this was obtained primarily in order to have information as to the behavior of the flicker photometer, irrespective of any theory as to its action, and part was obtained in order to test theoretical speculations. Taken together the data constitute a picture of the behavior of the flicker photometer probably more complete than any purely experimental study would be likely to afford. It is the purpose of this paper to assemble the data from the writer's various papers, presenting them in the form of a single chart. This chart may be considered either as an exposition of the characteristics of the flicker photometer sufficient for practical purposes, or as the body of facts which any theory of the instrument must explain.

Nature of the Chart

The chart of the flicker photometer consists of the extension to all working intensities of the diagram shown in Fig. 1, which is reproduced from an earlier paper,[1] which should be consulted for a full description of its significance. It shows the critical frequencies of disappearance of flicker for all ratios of illumination of the two alternating elements of the flicker field, starting with illumination of one element alone (e.g. by red light) and extending through all intermediate ratios to the illumination of the other element alone (e.g. by green light) under the condition that the sum of the two illuminations shall be constant. The

[1] A Polarization Flicker Photometer. Ives. Phil. Mag. April 1917, p. 360.

amounts of the two illuminations corresponding to any critical speed are shown in the lower diagram. Practically such a variation of relative illumination could be achieved by using two extended bright surfaces as the light sources, and arranging a variable diaphragm over each, the diaphragms being so connected that as one is opened the other is closed.

Examining Fig. 1—in which we shall confine our attention to the curved lines marked by circles—we see that at either end a high speed

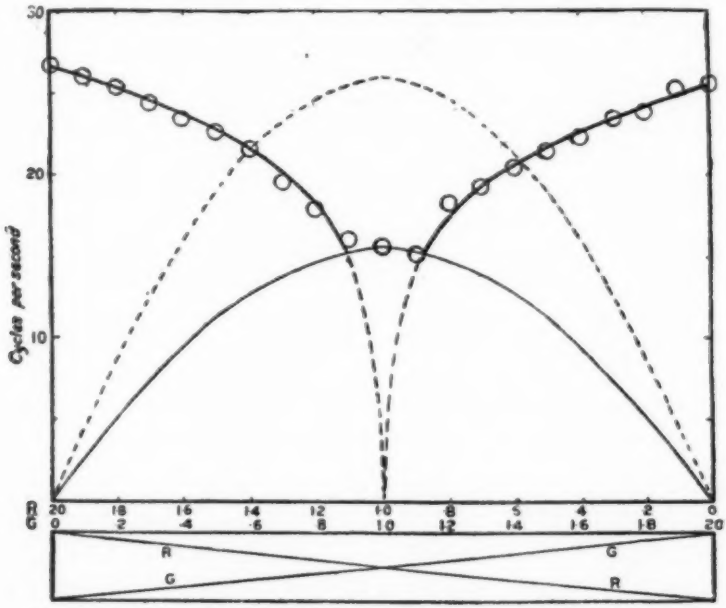

FIG. 1. *Critical speeds for disappearance of flicker for various relative amounts of alternated red and green light.*

of alternation is called for to abolish flicker; as the central portion of the diagram is approached the critical speed decreases, the two branches of the critical frequency curve descending toward zero. The critical speed does not however actually fall to zero (unless the two illuminations are of the same color) because of the occurrence of *color flicker*, or flicker still present when the two illuminations are equal in intensity but different in color. This lower limit to the critical frequency curve is shown by the approximately horizontal line joining the two descending branches of the critical frequency curve already discussed. The

region above the two descending branches and their connecting arm is a region in which no flicker occurs, while the region below is one in which flicker is present everywhere. The correct *speed* for operating the flicker photometer is the lowest possible which will not cause color flicker. The ratio of intensities which is evaluated as equality by the flicker photometer is that corresponding to the *mid-point* of the no-flicker region, which is found by oscillating the ratio of intensities between the two points of appearance of flicker. If the two branches of the critical frequency curve of Figure 1 are symmetrically placed about the equal illumination axis the flicker photometer setting is identical with the direct comparison or equality of brightness setting. If the branches are unsymmetrically placed, the ratio of intensities corresponding to the middle of the no-flicker region is no longer unity, i.e. the flicker photometer setting differs from the equality of brightness. The lower the color flicker critical speed and hence the lower the practical operating speed of the flicker photometer the narrower is the possible region of setting and hence the greater the precision.

The data incorporated in this diagram were obtained with the writer's polarization flicker photometer,[1] in which the transition from one color to the other is absolutely uniform, so that no question arises of flicker due to edges of discs or other mechanical imperfections. This is the only design of flicker photometer suitable for constructing a complete chart of the kind under discussion.

DATA AVAILABLE FOR CONSTRUCTION OF THE COMPLETE CHART

The experimental difficulties in the way of securing curves of the type of Fig. 1 with the polarization flicker photometer, extending over a wide range of intensities, were rather formidable, largely because so great a fraction of the available light was lost in the filtering and polarizing apparatus. With light sources now available higher brightnesses of the photometer field could be obtained so that it should be possible to complete the diagram experimentally, which would be highly desirable. However, by the use of data available from other studies, the gaps can be filled in well enough to make the result worth while.

Three sets of data will be used to complete the chart. The first set of data is shown in Fig. 2. It consists of critical frequency versus illumination data for various monochromatic radiations[2] for a large photometric field ($5° \times 8°$). The critical frequencies are in cycles per

[1] Studies in the Photometry of Lights of Different Colors. Ives, Phil. Mag. 1912, p. 149, 352, 744, 845, 853.

second; the illuminations are in arbitrary units, and are plotted on a logarithmic scale. The observations for red light lie on a single straight line, those for the other colors on broken lines, the slopes varying from color to color. The experimental data may be represented by equations of the form

$$\omega = a \log I + b$$

a and b each having one value for red light, and two, over different ranges of illumination, for each of the other colors.

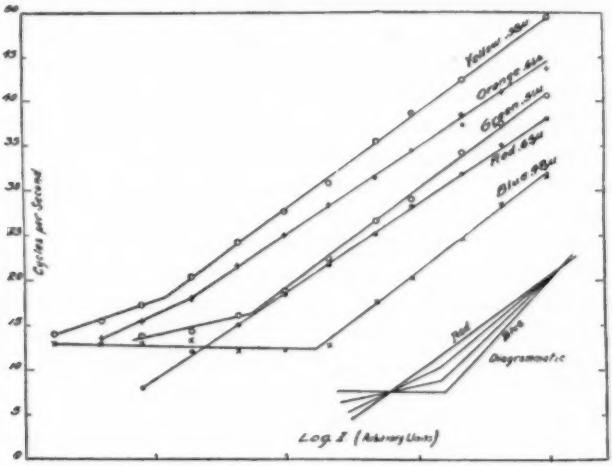

FIG. 2. *Critical frequency versus log illumination data for monochromatic radiations.*

The second set of data, also drawn from the paper on the polarization flicker photometer, consists of observations on the critical speeds of disappearance of color flicker, as compared with the critical speeds of the compared colors separately. The experimental points are shown in Fig. 3, where the upper line is the mean of the speeds for red and green, the colors studied; while the lower line, which is approximately straight, but of different slope, is drawn through the color flicker critical frequency observations.

The third set of data, taken from a recent paper on a theory of intermittent vision,[3] are embodied in the mathematical expression for the critical speeds for various amplitudes of the fluctuating stimulus. Calling a the amplitude, (excursion from the mean position, e.g. $a = \frac{1}{2}$ at the ends of the diagram, Fig. 1) it is shown in the paper quoted

[3] A Theory of Intermittent Vision. Ives, J. O. S. A. & R. S. I., June, 1922, p. 343.

that the critical speed ω, as the amplitude is changed, is represented by the equation:

$$\omega = a \log I\ a + b$$

where a is the same constant as in the previously quoted equation of the same form, and $[a \log a + b]$ corresponds to the b of the previous equation, that is, the equation for alternation of light with complete darkness is a special case of the equation just given. Now in the lower diagram of Fig. 1, representing the illuminations of the two alternated elements of the flicker photometer, the dovetailing of the two stimuli corresponds to a variation of the total (summed) amplitude from ½ at the ends, to zero at the center, so that the two constituent curves of Fig. 1 can be

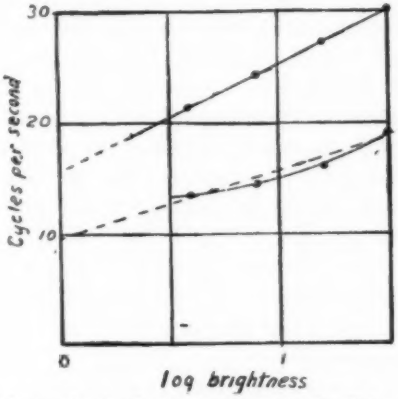

FIG. 3. *Critical frequencies for the disappearance of color flicker as compared with the mean critical frequencies for the alternated colors separately. Upper points, mean critical frequencies for red and green light. Lower points, critical frequencies for red and green alternated against each other.*

calculated from the experimentally established end points (Fig. 2). This expression is strictly applicable only where the dovetailed illuminations are of the same color, a point which will be discussed in the following section. Assuming that the use of this expression can be defended, as will be established, it is clear that we have available all the data necessary to build up the curves of Fig. 1 for all illuminations.

UTILIZATION OF THE DATA

In order to utilize the data above assembled, several steps are necessary. First of all the critical frequency data of Fig. 2 must be referred to a common scale of illumination, which is at least approxi-

mately correct, instead of the arbitrary scales used in obtaining the data. A rigidly correct scale of illumination, applicable to all the colors, could be assigned only upon agreement as to how we are to evaluate different colors photometrically. Avoiding a discussion of that problem we can secure the approximate scale sufficient for our present problem by noting that two straight lines of different slope, representing the critical frequencies for two colors, must cross *somewhere*, and that it is well established experimentally that critical frequencies for different colors are at least approximately the same for equal luminous values anywhere in the ordinary working range of illuminations. It has therefore been assumed that the red and green critical frequency-log I lines cross at 25 meter candles illumination of the flicker disc, and that the critical speed at this illumination is given by the constants in Porter's equation.[3] The choice of this point at 25 meter candles, which represents a practical working illumination, is in accord with considerable experimental evidence, but the exact point picked is not vital to the establishment of the main characteristics of the chart. On the basis of these assumptions, the equations of the lines of red and green light, which will be used for the chart are:

For red

$$\omega = 9.9 \log I_a + 39.1$$

For green, upper portion,

$$\omega = 11.05 \log I_a + 37.9$$

lower portion

$$\omega = 4.45 \log I_a + 24.9$$

The color flicker critical frequency line is for simplicity taken as the straight line most nearly fitting the experimental points established by Fig. 3. This stands in a proportional relation to the red and green critical frequency lines, which leads to its replotting on the assumed illumination scale according to the equation

$$\omega = 7.25 \log I + 22.5$$

These various lines are shown plotted to scale in Fig. 4.

There remains now the question of the applicability of the equation $\omega = a \log I_a + b$ where the amplitude is that resulting from the dovetailing of illuminations of unlike color. In general we note that the illuminations dovetailed call separately for different critical speeds. A lower critical speed pretty obviously means that the reaction produced in the eye makes smaller excursions from its mean position, that is, that it is of smaller amplitude, and vice versa. Consequently when two illuminations calling for different critical speeds are dovetailed the

hollows of the resultant fluctuating reaction will be lower, the peaks higher than if the illumination needing higher critical speed had been dovetailed with its own color.[4] Therefore, we may expect that the critical speeds called for by the above equation will in general be *too low for the higher branch* and *too high for the lower branch* of critical frequency curves such as that of Fig. 1, the error being progressively greater toward the center. Such differences in speed as the calculated branches indicate on either side of the center will therefore be somewhat less than they should be to correspond with the experimentally determined end points. It may be pointed out that this simply means that the center of the diagram corresponds to a somewhat smaller size of observing field than the ends. It does however correspond to *some* field size, which is sufficient for our present purpose.

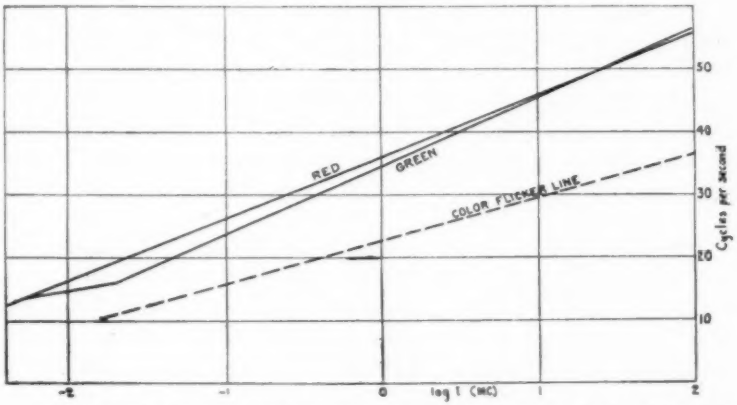

FIG. 4. *Critical frequency log illumination data for red and green light replotted to chosen illumination scale.*

THE CHART

Fig. 5 shows the complete chart, as constructed according to the above description, for red and green light. At the bottom are shown the relative amounts of the two stimuli which are dovetailed at the corresponding abscissae of the chart. At the sides of the chart are plotted red and green critical frequencies, the separations between successive points corresponding to equal distances along the log I axis

[4] This conception of the action of the flicker photometer as a producer of fluctuating reactions which differ in amplitude for the same intensity of stimulus according to the color and illumination level, is discussed at length in "The Theory of the Flicker Photometer" (Phil. Mag., November, 1914, p. 708).

of Fig. 4. Extending inward and downward from these points are the curves calculated by introducing the successive amplitudes ($a = \frac{1}{2}$ at

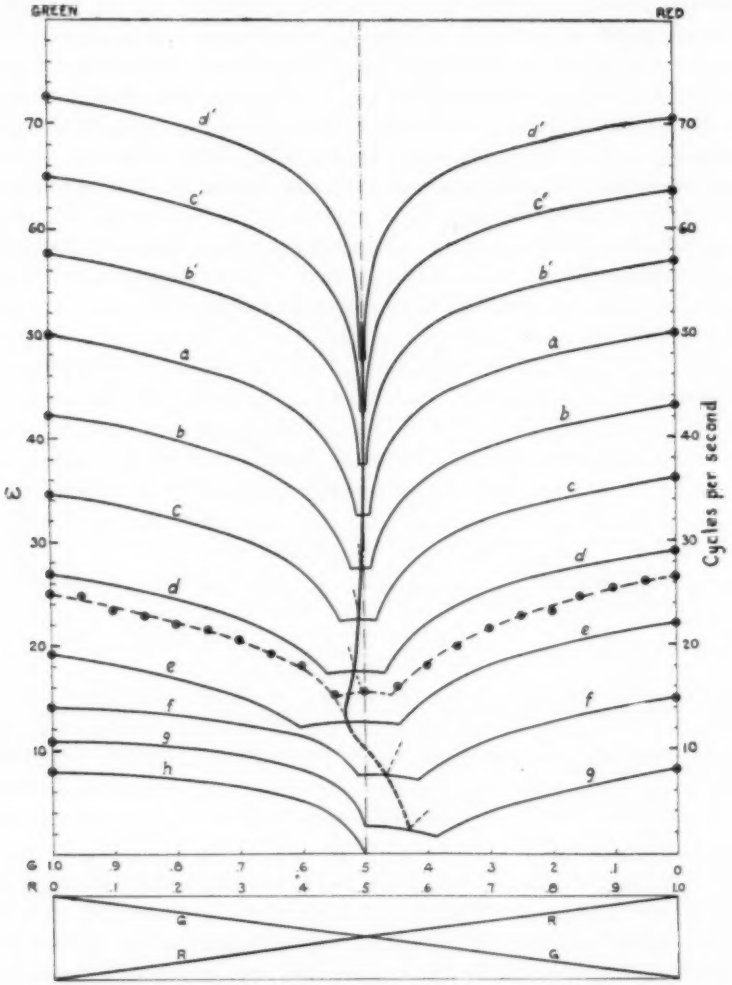

FIG. 5. *The chart of the flicker photometer. Heavy line close to vertical axis shows, by reference to the diagram of relative proportions at the bottom, the setting made with the flicker photometer at the illumination corresponding to the critical frequency curve cut.*

ends, and dropping to 0 at the center of the diagram) into the critical frequency—log I expressions for red and green respectively. These

curves are continued until they meet the approximately horizontal lines which are drawn through the critical frequencies for color flicker, also taken from Fig. 4. Each complete curve corresponding to one illumination therefore consists of two branches descending according to the logarithm of the amplitude, limited and connected by a short approximately horizontal branch. The various curves are lettered from *a*, corresponding to the condition of equal critical speeds for both colors, down to *h*, and upward by primed letters to *b'*, *c'*, *d'*. The experimentally obtained points of Fig. 1 are reproduced on the chart (circles); it will be seen that they fall very satisfactorily among the computed values. They show however much less dissymmetry, which is to be expected since the observing field was of much smaller diameter in the polarization flicker photometer than was the field used in obtaining the critical frequency data of Fig. 2.

Short dashed lines are drawn which bisect the no-flicker regions just above the limiting speeds for color flicker. These lines are the loci of the flicker photometer setting-positions for the speeds given by the corresponding ordinates. The heavy curved line closely hugging the axis of the figure connects the intersection of these dashed lines with the color-flicker critical-speed lines, that is, the points of most sensitive flicker setting.

Examining the chart in detail we note that it indicates a zig-zag course of the flicker setting about the axis of the figure as the illumination is progressively changed. At very high illuminations, at the top of the chart, the median of the flicker region is on the red side, that is, red will be underrated. At an illumination near but not exactly coincident with the equal critical speed point the flicker setting lies on the axis. On decreasing the illumination the setting point moves toward the green side, that is red will be overrated, constituting the *reversed Purkinje effect*, discovered by the writer.[2] At still lower illuminations, due to the change of slope of the green critical frequency-log illumination line the flicker setting point moves again toward the red side.

It is to be noted however that the most violent shift in position of the flicker photometer setting with change in illumination is indicated for the frequency region below about 12 cycles per second. No experimental observations have been made this low, and it is in fact doubtful whether the critical frequency relations here utilized still hold for those very low intensities. Moreover, the curves are computed on the basis of equal *physical* steps in intensity, neglecting the relatively greater

subjective judgment of short wave energy (the Purkinje effect) which would influence a photometric setting by direct comparison. The lack of complete consistency of the central portions of the computed curves with the end points, already alluded to, causes the lowest shift in direction of the flicker setting line to be displaced vertically, so that it does not correspond as nearly as it should to the locus of the second (lower) symmetrical critical-frequency curve. For these various reasons the lower end of the flicker setting curve has been drawn in as a dashed line only; it is useful as indicating the

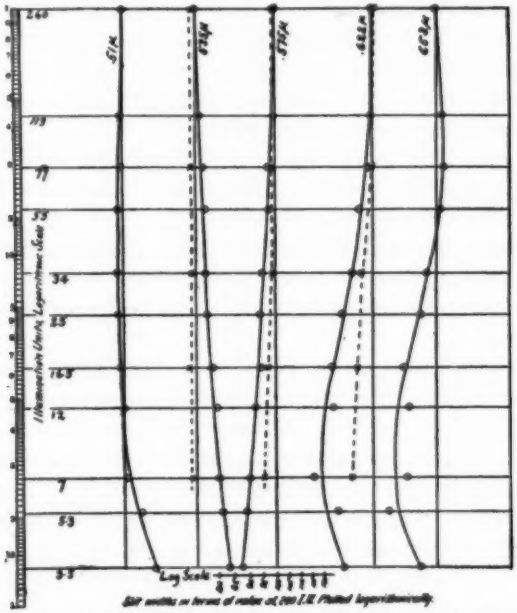

FIG. 6. *Experimental "slit-width" versus log illumination data for the flicker photometer.*

direction the curve is taking, but must not be taken too seriously as a quantitative guide.

A fact of importance to notice is that these shifts to either side of the axis are not of the same magnitude for the same (logarithmic) change of illumination. Because of the fact that the color-flicker critical-frequency drops below the homogeneous critical frequency by progressively greater amounts as the illumination increases, the two branches of the critical frequency-amplitude curves continue to relatively low values for the higher illuminations. Conversely at the lower

illuminations the greater relative values of the color-flicker critical frequencies prevent these curves from closely approaching the axis. As a net result the greatest variations of the flicker photometer setting from the axis occur at low illuminations; at high illuminations they are to a large extent offset by the narrowing of the flicker region near the setting point.

All of these findings are very beautifully checked by the experimental curves reproduced in Fig. 6 from an earlier paper of the writer.[2] In this figure the ordinates are illuminations (meter candles with field viewed through small artificial pupil) on a logarithmic scale, and so correspond to the critical frequency ordinate scale of Fig. 5, bearing in mind the logarithmic relation between illumination and critical frequency. In each case the colors alternated are a monochromatic spectrum patch and the "white" of a carbon lamp. This latter color, according to the findings of the study from which Fig. 3 is reproduced, yields critical frequency-illumination data practically coincident with green light. Consequently the "slit width" versus log illumination curves of Fig. 6 for red light should correspond to the case studied in the present paper. The qualitative corresponcence between Fig. 5 and 6 is in fact complete, showing the validity of the methods used in constructing the chart.

RESEARCH LABORATORIES OF THE
AMERICAN TELEPHONE AND TELEGRAPH CO.,
AND THE WESTERN ELECTRIC COMPANY, INC.
NOVEMBER 24, 1922.

On the Emission of Light by Canal Rays.—This article of Wien's consists mainly of equations developed from his conception of canal rays, which may be summarized as follows: (a) in a canal ray beam there are three kinds of particles; ionized atoms, neutral "unexcited" atoms and neutral "excited" atoms; (b) the relative proportions of these tend towards a statistical equilibrium, depending on the pressure of the gas which the beam is traversing; (c) the transitions of particles from one kind to another are similar to collisions between gas molecules, the "free time" or "free path" of a particle between transitions having values distributed exponentially about mean values corresponding to the mean free paths of gas molecules; (d) emission of light takes place when a particle passes from the neutral excited to the neutral unexcited state, and the mean value of the path preceding this transition is independent of the pressure of the gas; (e) but if a collision between a particle in the neutral excited state and a gas molecule occurs, the particle reverts to the neutral unexcited state without emission of light; (f) the mean free path preceding such a collision, and all the other kinds of mean free paths, are inversely as the pressure of the gas.

As Wien remarks, it will require an extensive research to test so elaborate a theory as this, and even to discriminate between the two possibilities that emission of light may be instantaneous, or may be spread exponentially over a perceptible time. The data now presented are curves showing the decrease in intensity of light emitted from a canal ray beam as it proceeds from a denser into a rarer gas, and the increase in intensity in the converse case. From the dependence of these curves on the pressure of the gas Wien concludes that the mean free path preceding a collision of type (e) is, for example, 1.66 mm and 2.58 mm for a hydrogen canal ray in nitrogen at .0041 and .003 mm Hg pressure, respectively. [W. Wien, (Munich) Ann. d. Phys. *70*, pp. 1-31; 1923.]

KARL K. DARROW

Spectroscopic Investigation of the Ionization of Argon by Electron Collisions.—Attempts to determine (by conventional methods) the electron-bombarding-voltages just sufficient to excite the "red spectrum" and the "blue spectrum" of argon, as detected by visual observation and by photography. The result the authors evidently hoped to establish was, that the red spectrum is excited when the argon atom is ionized (hence at the ionizing-voltage in a sparse electron-stream, or at the resonance-voltage in a dense electron-stream where there is ionization by cumulative action) and the blue spectrum when the argon atom is doubly ionized. On the whole, the observations can be interpreted to agree with this conception, provided that we take 11.5 volts for the resonance potential, 15 for the ionizing potential and 34 for the double ionization potential of argon. Thus, with "moderate" electron streams, the red spectrum disappears at 15 volts as the voltage is progressively diminished, while the blue spectrum appears at 19 volts and is perceptibly strengthened beyond 34 ($34=15+19$) volts as the voltage is increased. Measurements of total current and of partial currents show bends in the current-voltage curves at these voltages, indicating independently that ionization, direct or by cumulative action, is intensified at them. There are certain observations of which the explanation is rather forced; thus, the red spectrum persists down to 6.5 volts when a very dense electron stream is used, and the blue spectrum can be observed as far down as 11 volts; the authors can only suggest that the atoms previously ionized never have a chance to undergo complete restoration, the recombining electron being knocked out by a new impact before it get backs to the stable orbit. [F. Horton and A. C. Davies. Proc. Roy Soc., *102 A*, pp. 131-150; 1922.]

KARL K. DARROW

GEOMETRIC PROGRESSION IN OPTICALLY PREPARED STANDARDS

By Arthur P. Harrison

In an effort to prepare some permanent standards for colorimetric work a series of twenty-nine tubes was made from a solution of safranin, starting with a concentration just visible to the naked eye, and terminating in a color of definite strength. This darkest solution contained .0031% safranin.

The first tube was prepared by diluting .1 cc of this darkest color to 10 cc, and each following tube was prepared in such a way that the colors appeared to be increased just enough to be perceived by the unaided eye, so that a final set of tubes of equal gradation in color was obtained. The amounts of the strong safranin solution used were recorded and when a satisfactory set of standards was obtained this record was tabulated.

By analysis of this tabulated series, it was noticed that in order to make the tubes to differ perceptibly, it had been necessary to increase the strengths of safranin in each subsequent tube by an increasingly larger amount, verily approaching the appearance of a geometric series.

As this was so obvious it seemed at least interesting to calculate the quantities of safranin solution that would be required in a geometric series of twenty-nine items, starting with a quantity of .1 cc and ending in one of 10.0 cc.

In working for the factor in the series a, ar, ar^2, ar^3, ... ar^{n-1}, r was determined from the following equation: $r = \sqrt[n-1]{\frac{l}{a}}$ in which, r the factor, equals the $n-1$ root (28) of the last item (10.0 cc) divided by the first (0.1 cc), i. e.,

$$r = \sqrt[n-1]{\frac{l}{a}} = \sqrt[28]{\frac{10.0}{0.1}} = 1.179$$

The figures obtained by calculation and by observation are here compared.

The correlation of these two series is quite noticeable. Pairing the items, and applying Pearson's formula for the coefficient of correlation, $\frac{\Sigma\,(xy)}{n\,\sigma_1\,\sigma_2}$, in which Σ is the sum, x and y are the deviations from the average in the subject and relative variables, n the number of items and σ_1 and σ_2 the standard deviations of subject and relative, —we find the very close correlation of +.99, since perfect direct correlation by this formula is +1.0. A set of tubes prepared according to the

calculated figures proved as serviceable as the other and afforded the additional satisfaction of mathematical accuracy.

CC of A .0031% Safranin Solution Required in a Series of Tubes Graded by Amounts Sufficient to Produce a Color Change Perceptible to the Naked Eye.

Calculated to conform to a geometric series	Determined by observation*	Calculated to conform to a geometric series	Determined by observation*
.10	.10	1.20	1.25
.12		1.40	
.14	.15	1.65	1.50
.17		1.95	1.75
.20	.20		2.00
.23		2.30	2.25
.27	.25	2.70	2.50
.32	.30	3.15	2.75
.37	.35	3.70	3.00
.44	.40	4.35	3.25
.52	.45	5.15	3.50
.61	.50	6.10	4.00
.72	.75	7.20	4.50
.85		8.50	5.00
1.00	1.00	10.00	6.00
			7.00
			8.00
			9.00
			10.00

*The author is indebted to Mr. Scales of this Office for the original set of optically prepared safranin standards.

To see if this physiological phenomenon were true for other colors, solutions of luteol, methyl orange, malachite green, and Bismarck brown were made approximately of the same intensity as the safranin solution, and ten tubes of each of these solutions prepared using the safranin figures, 1.00 to 4.35, and the geometric relationship verified. The strengths of the colors used were as follows: safranin .0031%, luteol .006%, methyl orange .005%, malachite green .0015%, Bismarck brown .003%.

BUREAU OF PLANT INDUSTRY,
WASHINGTON, D. C.

INSTRUMENT SECTION

A DEVICE FOR LOGARITHMIC AND SEMI-LOGARITHMIC PLOTTING AND FINDING POWERS AND EXPONENTIALS

By R. A. Castleman, Jr.

Abstract

In much laboratory work simultaneous observations are made on two dependent quantities, all others being kept constant. A relation is then sought between these quantities. One of the first recourses is to logarithmic and semi-logarithmic plotting. By dimensional reasoning, relations involving other quantities may then often be inferred, even without further experimentation. A device that combines speed, accuracy, and simplicity for this sort of plotting is therefore desirable as a laboratory adjunct.

In this paper the theory of logarithmic and semi-logarithmic plotting is reviewed, and a device is described which, it is thought, meets the above demands.

The theory of power and exponential finding, especially as the inverse of logarithmic and semi-logarithmic plotting, respectively, is also reviewed, and a simple addition to the above apparatus is described, by which one can read powers and exponentials.

Theory

The theory of logarithmic plotting is as follows:

Given an equation—

$$y = ax^n \tag{1}$$

or

$$\log y = \log a + n \log x \tag{2}$$

Plotted on *log y* and *log x* axes, (2) is a straight line with slope $= n$ and *log y* intercept $=$ *log a*. Hence if a series of simultaneous values of x and y, when plotted against each other logarithmically, fall on a straight line, the equation connecting them is of form (1). The value of n is the slope of this line with reference to the *log x* axis. "a" is the value of "y" when $x = 1$, or *log a* is the value of *log y* when *log x* $= 0$.

The theory of semi-logarithmic plotting is as follows:

Given an equation of form—

$$y = a\ 10^{mx} \tag{3}$$

or

$$y = ae^{nx} \tag{4}$$

Taking logarithms

$$\log_{10} y = \log_{10} a + mx \tag{5}$$

or

$$\log_e y = \log_e a + nx \tag{6}$$

$$\left(\text{Note that } \quad n = \frac{m}{.4343}\right)$$

On *log y* and x axes (5) is a straight line with slope $= m$ and *log y* intercept $=$ *log a*. If, now, for a given set of simultaneous values of x and y,

$\log_{10} y$ be plotted against x, and a straight line results, the quantities are interrelated by an equation of form (3) and the value of m is the slope of the line with reference to the X axis. *Log a* is the value of *log y* when $x = o$.

One method of solving data according to the above theory is to plot the logarithms of the corresponding quantities against each other on uniform cross-section paper. The slope of the line is then found by finding the ordinate distance, $y_2 - y_1$, between any two convenient points on the line, and the abscissa distance, $x_2 - x_1$, between the same two points, both distances being measured in units of the cross-section paper.

Then

$$n = \frac{y_2 - y_1}{x_2 - x_1} \tag{7}$$

and "a" is the antilog of the value of *log y* when *log* $x = 0$. A second method is by the use of "logarithmic plotting paper." This paper is similar to ordinary cross-section paper, except that the lines, instead of being uniformly spaced, are at distances from the initial line proportional to the logarithms of the numbers to which said lines correspond. This is quite equivalent to the method outlined above. The slope must be measured with the assistance of a *uniform* scale. The value of "a" is the y-intercept on the $x = 1$ line.

A third method is as follows: If two logarithmic scales are capable of mutual relative motion, while being held so as to be always mutually at right angles, then when the reading on the horizontal scale is x, while that on the vertical scale is y, the point thus determined has co-ordinates *log x* and *log y*. By continuing this process with the other pairs of values of x and y the logarithmic plotting can be accomplished.

Semi-logarithmic plotting can be accomplished in a manner quite analogous to that outlined above for logarithmic plotting. In preparing semi-log plotting paper, care should be taken that unity on the log scale—i.e., 1 to 10, 10 to 100, etc.,—be made equal to some simple multiple, "k", of the straight scale divisions. Then if the slope is measured with a uniform scale, and a Briggsian table has been used in making the log scale,—

$$y = a \cdot 10^{mx} \tag{3}$$

where $$m = \frac{\text{Slope}}{k}$$

and a = value of y when $x = 0$.

(3) can be transformed into the form

$$y = ae^{nx} \tag{4}$$

by dividing "m" by .4343

The theory of finding a power of a number is as follows:

Let $$y = x^n \tag{8}$$

Then $$\log y = n \log x \tag{9}$$

To evaluate x^n, then, we must multiply *log* x by n and find the antilog of the result. There are three methods of doing this: (1) by a logarithm table; (2) by a *log log* rule; (3) by rectangulation. (1) is tedious and often complicated; (2) accomplishes the multiplication by applying simple Mannheim rule computation to *log* x and n,—one scale is proportional to *log* n and the other to *log log* x. This form of apparatus has two decided liabilities, which are evident on inspection: (a) A very uneven distribution of accuracy, due to the fact that the rate of change of the *log log* of small numbers is much greater than that of large numbers. (b) The *log log* rule is direct reading for only a narrow range of values of n and of x,—viz., positive values of n and of *log* x. In all other cases at least one reciprocal must be found.

The solution by rectangulation is as follows: If one leg of a right triangle, whose hypothenuse has a slope "n" with respect to said leg, be made equal to *log* x, the other leg is equal to n *log* x.

The theory of exponential-finding is as follows:

Let $$y = 10^{mx} \tag{10}$$

Then $$\log_{10} y = mx \tag{11}$$

To evaluate 10^{mx}, then, we must multiply x by m and take the Briggsian antilog of the result. This can be accomplished (1) by a log table; (2) by rectangulation. The solution by rectangulation is: If one leg of a right triangle, whose hypothenuse has a slope m with respect to said leg, be made equal to x, the other leg is equal to mx. If, now, scales run along the two legs, said scales being so constructed that distances along the latter are Briggsian logarithms of corresponding distances along the former, while being marked with their antilogarithms, the reading on the latter scale, when that on the former is x, is 10^{mx}. To evaluate e^{mx}, we proceed as above, except that the relation between the two scales is that of the Naperian system.

It should be noted that the operation of power-finding is inverse to that of logarithmic plotting, while the operation of exponential-finding is inverse to that of semi-logarithmic plotting.

DESCRIPTION OF APPARATUS

The backbone of the apparatus is a two-faced member such as a drawing board. One side of this member is designed for plotting, the other side for power and exponential finding. For convenience the latter side will be described first.

APPARATUS FOR POWER AND EXPONENTIAL-FINDING

(This is illustrated in Fig. 1, to which the letters in the following description refer.)

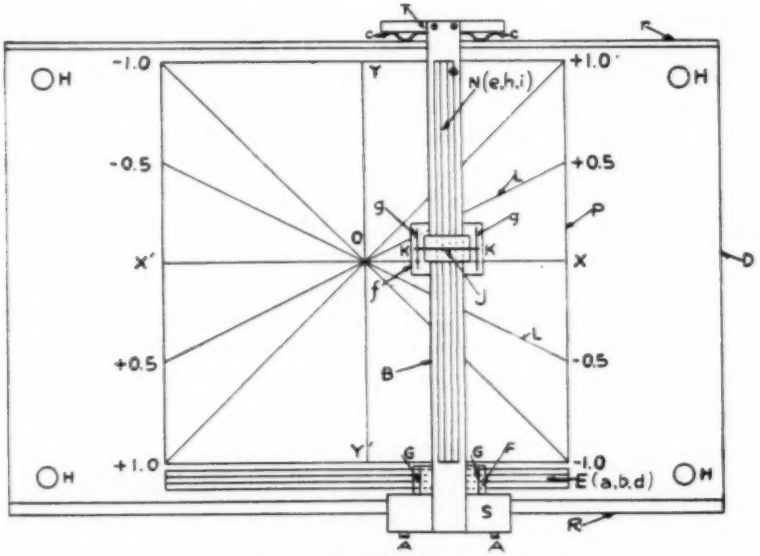

FIG. 1. *Power and exponential finding apparatus.*

The essential part of the apparatus is a member "*D*," to two opposite ends of which, and parallel to each other, are attached rails "*R*" and "*r*." Shoes "*S*" and "*T*" ride on "*R*" and "*r*," respectively. Between "*S*" and "*T*" is stretched a member "*B*," similar to the blade on a T-square. Centrally to the board is fastened a member "*P*," such as a sheet of paper, celluloid, or other suitable material. This member "*P*" is divided into four quadrants, the *X*- and *Y*- axes being parallel and perpendicular, respectively, to "*R*." Through the origin "*O*" are drawn lines of various slopes, each line being marked with the value (n) of its slope with respect to the *X*- axis. Screws "*A*" on "*S*" provide

means for adjusting "*B*" perpendicular to "*R*," and springs "*c*" on "*T*" provide retention of this perpendicularity and insure smooth working. Rubber buffers "*H*" protect the working parts from the table while using the other face of the board.

Scales "*E*" run along the bottom of the board, parallel to "*R*." One of these scales, "*a*," is logarithmic, and two are uniform. Scale "*a*" contains two units, each being equal to the distance $X'O = OX$. The uniform scales are constructed as follows: Distances along one uniform scale, "*b*," are Briggsian antilogarithms of equal distances along scale "*a*," while distances along the other, "*d*," are Naperian antilogarithms of these latter. The zeros of scales "*b*" and "*d*" and the "*1*" of scale "*a*" lie along the line YOY'.

Similar scales "*N*" run up the blade "*B*." Of these "*e*" is logarithmic and "*h*" and "*i*" are uniform. The "*1*" of scale "*e*" and the zeros of scales "*h*" and "*i*" lie along XOX'.

The shoe "*S*" has an indicator "*F*" of transparent material (e.g., xylonite) on the lower face of which and at equal distances from the edges of the blade "*B*" are drawn lines "*G*," to be used as indices for the scales "E." Along the blade "*B*" runs a slider "*f*" of transparent material. On the lower faces of the sides of this slider and immediately above the lines "*G*" are drawn lines "*g*." Across the lower face of the central part of the slider is drawn a line "*J*" which line is extended to meet the lines "*g*" at points "*K*." The line "*J*" is index to the scales "*N*," the points "*K*" are indices to the slope-lines "*L*," and the lines "*G*" are indices to the scales "E."

MANIPULATION

(a) Power-finding: Set "G" at x on scale "a," "K" at n (the slope of some line *L*) and read x^n at the point of intersection of "J" with scale "e."

(b) Exponential-finding: (1) Evaluating 10^{nx}. Set "G" at x on scale "b," "K" at n (as above) and read 10^{nx} at the point of intersection of "J" with scale "e." (2) Evaluating e^{nx}. Set "G" at x on scale "d," "K" at n (as above) and read e^{nx} at the point of intersection of "J" with scale "e."

The following points are to be noted: (1) Interpolation for n is linear in the vertical direction, and can be best accomplished with the assistance of the uniform scales "h" or "i." (2) The value of x^n can be read directly, whether x be fractional or integral, and whether n

be positive or negative. (2) The value of 10^{nx} or e^{nx} can be read directly, whether x or n be positive or negative.

APPARATUS FOR LOGARITHMIC AND SEMI-LOGARITHMIC PLOTTING

This apparatus, illustrated in detail in Figure Two, is so similar to that described above for power and exponential finding, that this description need not be repeated. The only difference is the absence of the member "P," and the difference in the design of the slider. This latter has, besides the lines "g" and "J," as above, pencil holes "q" which lie at the intersection of a line "Q," drawn on the lower surface of the slider, with the lines "g."

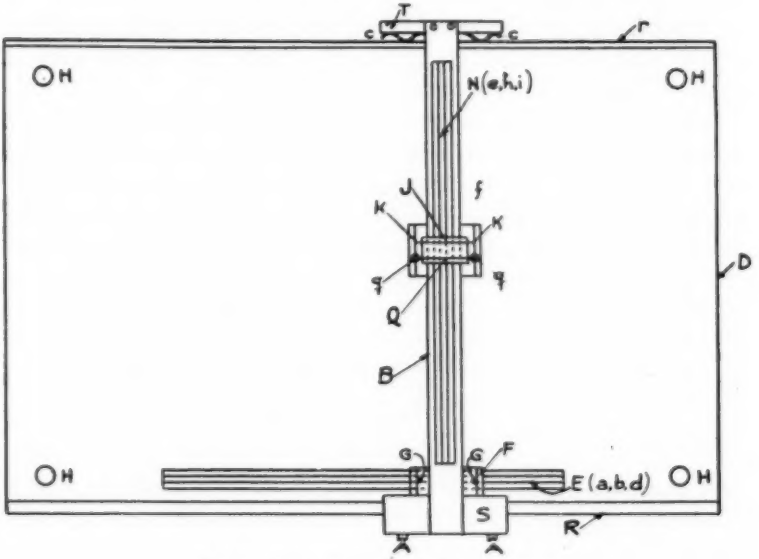

FIG. 2. *Log and semi-log plotting apparatus.*

MANIPULATION

(1) Logarithmic plotting. Set the index "G" at x on scale "a," set the index "Q" at y on scale "e," and mark through "q." (Note that this is ordinary Cartesian plotting of *log* y vs. *log* x.) When all the data have thus been plotted draw a straight line through these points, if possible. Determine the slope n of this line by means of equation (7) above, with the assistance of the uniform scales, and the indices "G" and "J." Note that if the X- interval is made equal to

10, the Y- interval, with its decimal point moved one to the left, gives the value of n. The reading of y when $x=1$ gives the value of a of equation (1).

(2) Semi-logarithmic plotting is accomplished in a similar manner, except that scale "b" or "d" is used in conjunction with scale "e," or scale "a" in conjunction with "h" or "i." The a of equation (3) is the reading of y at $x=0$.

(3) To determine simultaneous values of x and y when these are interrelated by an equation of form (1), we proceed as follows: We are given a and n. We set "G" at 1 on scale "a," "Q" at the value of a on scale "e" and mark through "q." This gives the point (1, a). Through this point, with the assistance of the *uniform* scales "b" and "h," or "d" and "i," we erect a line of slope n. Finally by means of the indices "G," "J," and "K," etc., we read simultaneous values of y and x.

(4) An analogous procedure suffices for an equation of form (3).

Specific examples of applications of the above described apparatus are without the scope of the present paper, but will be apparent to those initiated in laboratory, engineering, and design work.

EAST FALLS CHURCH, VA.

Excitation and Ionization Potentials of Helium.—Previously published measurements by Franck and Knipping gave a series of resonance potentials at 20.45, 21.25, 21.9 and 23.6 volts and ionization at 25.3 volts. Results of others notably Horton and Davis were in substantial agreement with this. Recently Lyman has obtained photographs of the helium spectrum which show a series of lines starting at $\lambda=584.4$ A with a limit $\lambda=502$ A and a fainter line at $\lambda=600.5$. The limiting frequency gives a value .8 volts lower than the observed ionization potential. The discrepancy is ascribed to a misinterpretation of measurements.

The procedure was to measure the difference between the least potential required to excite radiation and that potential at which an electron could produce two successive radiation collisions. This interval, 20.45 volts, was assumed to be the lowest potential in computing the above values. Evidence is now given that it is in fact the second potential, for of the two types of collision the second is more probable than the first. Under the experimental conditions the probability of two successive collisions of the first type may be very small compared with the chance of two of which one is of one type and one of the other. The potentials recomputed on this basis are interpreted as follows:

Series	Volts Observed	Remarks
$1S-2s$	19.75	Formation of metastable helium Radiation only as result of impurities
$1S-2S$	20.55	Lyman line $\lambda=600$. Emission contrary to selection principle
$1S-2P$	21.2	Lyman series
$1S-3P$	22.9	
$1S$	24.6	Series Limit. Ionization

The agreement of the above is all within .1 volt of values computed from the spectral data. Other measurements of Franck and his associates based on the value of the helium point have been revised. A table showing the new values for H_2, N_2 the hydrogen halides and *HCN* is given. The revised data are in almost exact agreement with the measurements of Mohler and Foote. In spite of the satisfactory numerical agreement it must be noted that the experimental results of Horton and Davies can not be accounted for in the same manner. The latter also differ in their interpretation of results particularly as concerns the lowest potential. The explanation of the second potential as well as the first offer interesting possibilities for further experimental work. [J. Franck. ZS. f. Phys., *11*, p. 155; 1922.] F. L. MOHLER

Excitation of Characteristic X-rays from Light Elements.—Experiments were performed on Li, Be, and B (the 3d, 4th and 5th elements of the periodic table) by the conventional method—a target made of the substance under test is subjected to electron bombardment; measurements are made on the bombarding voltage and on the photo-electric emission from a plate exposed to whatever radiation may come from the target, the latter quantity is plotted against the former, and wherever the curve has a distinguishable sudden upturn (going in the sense of increasing voltages) it is deduced that the voltage is just sufficient to excite radiation. The data given are: Li 12.0, 31.8 and 37.0 volts; Be 16.0, 20.3, 78.2 and 93 volts; B 23.45, 27.92 and 147.5 volts. The authors introduce the novel interpretation that some of these may correspond, not to critical absorption frequencies but to emission frequencies; or, in another terminology, that some of them may be resonance potentials and not ionization potentials. Thus the voltages 37.0 and 31.8 of Li stand approximately in the ratio 32:27, like the first two members of the Lyman series; and the voltages 20.3 and 16.0 of Be, likewise the voltages 27.92 and 23.45 of B, are approximately as 27:20, like the first two members of the Balmer series. If this interpretation is correct, then (for example) 31.8 and 37.0 are respectively the voltages required to drive a *K*-electron of Li from its stable orbit to the first and second outward-lying virtual orbits, and the true *K* critical absorption frequency, i.e. the ionizing frequency, of Li corresponds to a still higher voltage 42.2. For the true *K* and *L* critical absorption frequencies the authors calculate: Li, 42.2 and 12 (volts); Be, 104.3 and 28.8; B, 148 and 42.2. [J. C. McLennan and M. L. Clark. Toronto. Proc. Roy. Soc., *102 A*, pp. 389-410; 1923.]

K. K. DARROW

A PROJECTION ELECTROSCOPE FOR MEASUREMENTS IN RADIOACTIVITY

By Howard M. Elsey

The existing types of electroscopes have been designed primarily for laboratory use in accurately measuring the radioactivity of different substances and are not readily adapted to demonstrate experiments to a large audience. It is true that one of these instruments may be placed in front of a projection lantern and an image of the leaf thus thrown on the screen. However, such a use is only a makeshift and it was thought desirable to design an electroscope which might take the place of the slide carrier on a projection lantern.

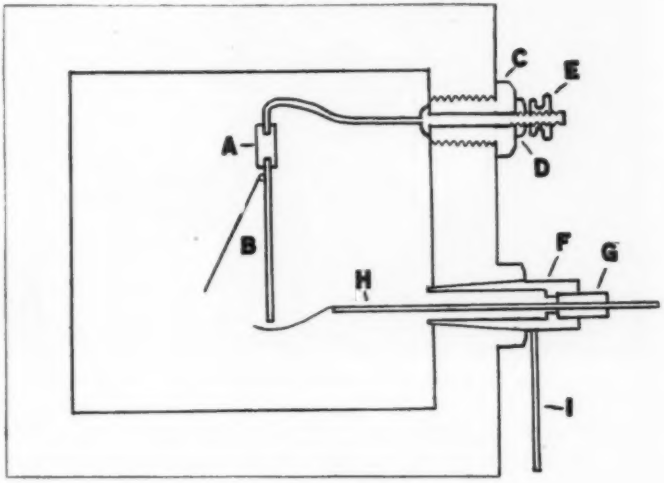

Fig. 1. *Diagram of projection electroscope.*

In Fig. 1, a diagram of such an instrument is shown. The frame is of heavy brass, lined with lead, and the front and back, which are not shown, are also of brass lined with lead. B is the gold leaf system which is attached to the amber insulation A which in turn is fastened to a brass rod. This rod extends through the case passing through a hollow nut C, which is sufficiently large so that when the nut D is loosened, C may be screwed out leaving a hole through which the leaf

system may be removed. The leaf system may be charged by bringing the wire on the end of the rod H in contact with the bottom of the brass rod of the leaf system.

This rod H passes out to the exterior through the amber insulation G. This insulation is cemented into a tapered sleeve F and by means of the handle I the sleeve may be rotated to bring the wire on H in contact or out of contact with the system B. After charging B, if contact is then broken with H, the instrument becomes a gamma ray electroscope. With H in contact with B, the instrument may be used as an alpha or beta ray electroscope and by connecting the outer end of H with the insulated electrode of an emanation chamber, the instrument becomes an ordinary emanation electroscope.

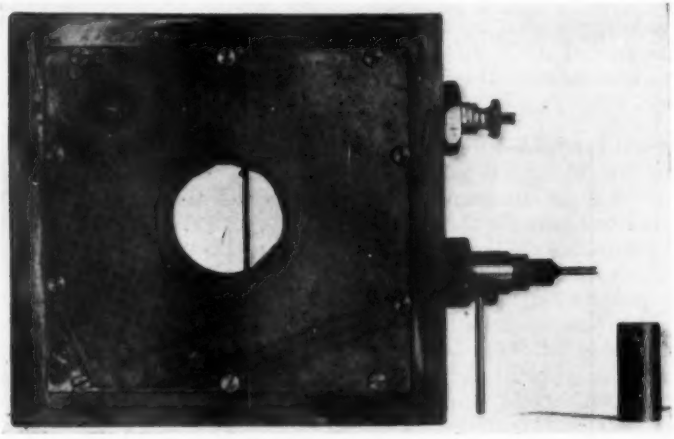

FIG. 2. *Projection electroscope.*

A picture of the assembled instrument is shown in Fig. 2. The windows on the instrument are of sheet mica, the outside surfaces being covered with a very thin coat of glycerine to prevent the accumulation of charges which might attract the leaf. In case the leaf does touch the windows through careless handling, it does not stick as badly to mica as to glass and a sample of radioactive material brought near the window will cause it to quickly fall away.

By cementing a transparent scale on one of the electroscope windows, the instrument may be readily converted into a quantitative one with which surprisingly accurate measurements may be made without the nervous strain which follows the continued use of the Tele microscope.

In Fig. 3 is shown a simpler form of the instrument with but a single amber insulation at A. By covering the threaded collar B with a lead lined cap, this instrument may be converted into a gamma ray electroscope. Although much simpler in design and thus easier to use, the larger capacity of the leaf system renders this instrument much less sensitive than the first form which is an exceedingly sensitive one.

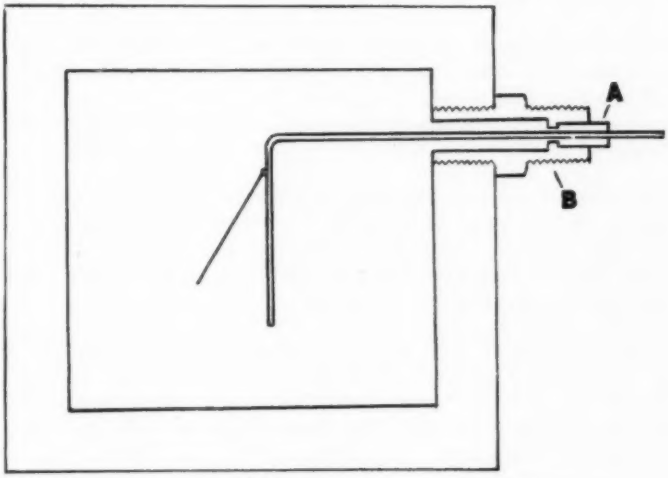

FIG. 3. *Diagram of simpler form of projection electroscope.*

Each of these two types have been prepared and used very successfully in demonstrating experiments to large classes.

A third modification, which has not been tried but which undoubtedly would be successful, would retain all the sensitivity of the first type and yet would be some simpler in construction. In this form, the leaf system would be fastened to a large brass screw let into the top of the case, the head being countersunk to not interfere with the entrance of the instrument into the lantern.

DEPARTMENT OF CHEMISTRY,
UNIVERSITY OF KANSAS,
LAWRENCE, KANSAS.
FEBRUARY 8, 1923.

Absorption of 5460.97A by Luminous Mercury Vapor.—A long straight tube is equipped with several lateral mercury electrodes, and an arc is operated between two of them towards one end of the tube, while a high-voltage low-current transformer discharge is passed between two others at the other end; the light emitted from the arc and travelling down the tube passes through the layer of mercury vapor excited by the transformer discharge, and thence into the spectroscope. The results indicate that of the twelve components which make up the mercury green "line," three (the one at 5460.97A, and its two neighbours) are absorbed by mercury vapor subject to the particular kind of excitation here described. (The demonstration is not quite binding, for the resolving power of the optical system used was such that the innermost five components were merged into a single bright band, the central part of which was darkened by the absorption, while the edges and the outer components were relatively unaffected; the width of the darkened band indicates that the three middle components were effaced.) On splitting the green line into 9 components by applying a strong magnetic field and sighting transversely to the field, it was found that only the central component of the 9 was absorbed by the vapor excited by the transformer discharge.

Are the different components of the green line due to different isotopes of mercury? The separations between them are much larger than those predicted from the Bohr theory; but if we multiply the predicted separations by the atomic number of mercury, we get figures agreeing more or less with the separations of the four nearest-central components from the central one. The same device lately brought a similar success with the red lithium line. [J. C. McLennan, D. S. Ainslie, and F. M. Cale. Proc. Roy. Soc., *102A*, p. 33-45; 1922.]

K. K. DARROW

Destruction of the Polarization of Resonance-Radiation by Weak Magnetic Fields.—R. W. Wood reports in a recent issue of Nature that he has discovered a pronounced influence of magnetic field upon the polarization of the resonance radiation of wave-length 2536 from mercury vapor, which must have affected his and other previous experiments. Magnetic field, it is found, reduces the polarization of the resonance radiation excited by incident polarized light of the same wave length 2536, if the field is parallel to the magnetic vector and normal to the direction of propagation of the exciting light. The percentage of polarization is 90% in the absence of magnetic field and is reduced to 50% by the earth's magnetic field alone, and is practically annulled by a field five or six times stronger. Lord Rayleigh's observation, of the variation of degree of polarization along the path of the exciting beam, may have resulted from the magnetic fields applied at various points of his apparatus. In any case this appears to be a new magneto-optic effect. [R. W. Wood and A. Ellett. Nature *111*, p. 255, February 24, 1923; Science, *57*, pp. 267-268, March 2, 1923.]

KARL K. DARROW

A PRECISE METHOD OF MEASURING SMALL EMFS AND THE CHANGE IN THERMOELECTRIC POWER OF TIN AT THE MELTING POINT

By T. R. Harrison and Paul D. Foote

The investigation of the relation of thermoelectric power of a metal in the solid and liquid phases is of interest from the standpoint of electronic theory. Although considerable work has been published in this regard by several investigators, many of the results are contradictory and the experimental methods have been rather unsatisfactory, especially for tin. Weiss and Koenigsberger[1] observed a sudden change in the thermoelectric power of a tin-constantan thermocouple amounting to 8.8 microvolts/deg C at the melting point of tin. Koenigsberger,[2] from a consideration of his own work and the work of others, concluded that the thermoelectric power of liquid tin is about 5 microvolts/deg greater than that of solid tin. Cermak and Schmidt[3] found no difference thermoelectrically between solid and liquid tin at the melting point while Siebel[4] observed a difference of from 2 to 2.7 microvolts/deg. Darling and Grace[5] concluded that there is no discontinuous change in the thermoelectric power of a tin-metal thermocouple at the melting point of tin. This result was corroborated by Pelabon[6] but the precision of the latter work was very evidently insufficient to permit even the detection of an effect as small as that to be expected.

The object of the present investigation has been to measure, by a method capable of higher precision than that heretofore employed, the change in thermoelectric power of a platinum-10% rhodium versus tin thermocouple in the vicinity of the tin melting point, using tin[7] of purity 99.988%. Special attention has been given to the investigation of the abruptness of the transition.

The method is illustrated by Fig. 1. A pyrex glass tube, 75 cm in length, having an inside diameter of about 5 mm in the upper portion and about 2 mm in the lower portion was filled with tin. The upper

[1] Weiss and Koenigsberger, Ann. d. Phys., (4) *35*, p. 21; 1911.
[2] Koenigsberger, Ann. d. Phys., (4) *47*, p. 563; 1915.
[3] Cermak and Schmidt, Ann. d. Phys. (4) *36*, p. 579; 1911.
[4] Siebel, Inaug. Diss., Kiel; 1914.
[5] Darling and Grace, Proc. Lond. Phys. Soc., *30*, p. 14; 1917.
[6] Pelabon, Ann. de Physique *13*, p. 169; 1920.
[7] Bureau of Standards Circular No. 66, p. 6.

part of the tube was electrically heated so that the temperature could be controlled to within 0.01°C. A Pt-PtRh thermocouple, *A*, was protected by pyrex glass tubes which were fused together into a single piece about 1.5 mm in diameter, only one side of the extreme junction of the couple being exposed to the tin. The lower part of the main tube

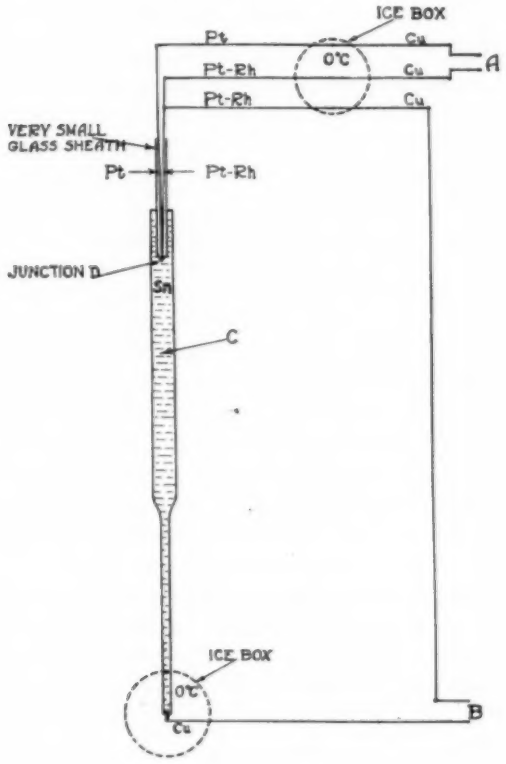

FIG. 1. *Arrangement of couples.*

was immersed in an ice-bath, copper wire making contact with the solid tin. The PtRh wire of couple *A*, in conjunction with the tin, formed the experimental couple under investigation. The emf developed by couple *A* furnishes a measurement of the temperature, t°C, of the hot junction *D*, which is also the hot junction of the Sn-PtRh couple *B*, both couples having a cold junction temperature of 0°C.

Let t°C be above the melting point of tin. A surface *C*, will then exist which defines the boundary between liquid and solid tin. This surface will have the temperature 231.9°C, the melting point of the pure material employed. The emf measured at *B* will then be equivalent to that of a PtRh-Solid Tin couple with a cold junction at 0°C and a hot junction at 231.9°C in series with a PtRh-Liquid Tin couple with a cold junction at 231.9°C and a hot junction at t°C. The emf of this first couple remains fixed in value so that the total emf is that of the second couple plus a constant. Hence the slope $\frac{de}{dt}$ of the emf-temperature curve for the compound couple is the thermoelectric power of the PtRh alloy versus Liquid Tin. When t is less than 231.9, the slope of the emf-temperature curve is the thermoelectric power of PtRh versus Solid Tin. The difference between these two slopes at 231.9°C is the thermoelectric power of Solid Tin versus Liquid Tin at the melting point. This, as will appear, shortly, is of the order of one microvolt per degree centigrade, the value, of course, being independent of the kind of metal with which the tin is compared.

It is obvious that in order to determine whether the change takes place over a small range of temperature or abruptly at the melting point, it was necessary to measure the emf with a precision of 0.1 microvolt or better at many temperatures within a narrow range above and below the melting point.

Considerable work of a preliminary nature was carried on over a period of two years. In the earlier experiments iron was selected for the comparison metal because of its freedom from alloying with tin at the temperatures employed. The results were not consistent however because of the slight inhomogeneity of iron wires and in part because of the potentiometric system used in these early measurements.

The preliminary data however showed that tin near the melting point has a very small thermoelectric power when referred to copper, to gold or to the alloy Pt-10%Rh. The latter material proved especially advantageous since very homogeneous wires of 0.1 mm diameter may be readily drawn and since contamination by tin is very slight at low temperatures.

With the cold junctions at 0°C, the emf of the PtRh-Sn couple rises slowly to a maximum value of 0.383 millivolts at the melting point of tin, and then decreases at approximately the same rate with further increase in temperature. Thus the required precision of 0.1 microvolt

demands an emf measurement which need not be more precise than to one part in 4,000. Furthermore the thermoelectric power of this couple is so low (roughly half the total effect sought) that sufficiently accurate temperature measurements are readily made.

The small value of the maximum emf observed permitted, and the required precision of 0.1 microvolt necessitated, the employment of special devices designed to reduce and eliminate parasitic emfs in the circuit. The greater part of the stray emfs may be eliminated by the usual method of reversals but irregular effects in keys or non-reversible emfs in parts of the switches are not so easily removed.

A special rotary selective switch having thin PtRh contact strips was constructed and arranged for maintenance at a uniform temperature. This switch with its clean surfaces formed the only connections in the entire thermoelectric circuit which were not fused or soldered. The switch was mounted on the lower side of a brass disk. Around the switch on a small metal, cylindrical shell were wound the three sections of "Therlo" resistance wire, r_1, r_2 and r_3 of Fig. 2. These

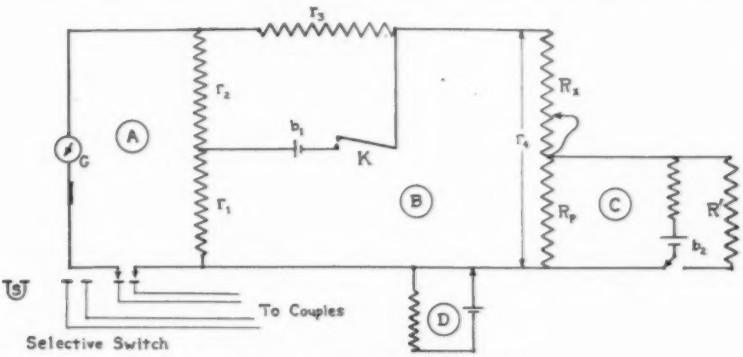

FIG. 2. *Diagram of electrical circuit.*

resistances were connected by hard solder to the copper in-lead wires. A variable current, adjusted so that the potential drop across coils r_1 and r_2 balanced the emf of the couple, was a measure of the emf of the couple. This brass disk formed the cover of a cylindrical brass box which protected the above mentioned parts and could be placed near the bottom of a Dewar flask filled with water and serving as a bath of uniform temperature. The copper wires were brought out through long thin German silver tubes. A similar tube with a handle on one end passed through a slightly larger tube for operating the switch. A

locking device at the switch handle made it necessary to push the handle down before turning, thus opening the contacts and providing entire selectivity or reversibility without interference from other contacts.

By this construction the fundamental thermoelectric circuit *A*, Fig. 2, was kept unusually free from extraneous emfs, the leads from the selective switch to the respective couples and the galvanometer leads being carefully matched thermoelectrically.

The measured variable current was obtained from a Disselhorst potentiometer, use being made of the deflection potentiometer principle which for the present purpose may be stated as follows. If the emf terminals of any potentiometer are connected to a source of zero emf having zero resistance (short-circuited), the proper keys and switches being closed, and if the resistance of the galvanometer circuit, including the resistance through the potentiometer, is adjusted to the value for which the galvanometer is calibrated to read emf, then the galvanometer reading will be the same as the emf value indicated by the setting of the potentiometer dials, provided the potentiometer battery current was properly balanced against a standard cell when the extra current is not being drawn through the galvanometer. In other words, under the stated conditions, a current will flow through the galvanometer the strength of which equals the emf indicated by the dial settings divided by the total resistance of the galvanometer circuit. Coils r_1, r_2 and r_3 are connected, in series with an adjustable resistance R_x, to the proper terminals of the potentiometer replacing the galvanometer referred to above.

By connecting a battery b_1 and key K as shown in Fig. 2, circuit *B* constitutes a wheatstone bridge. The adjustment of R_x to balance the bridge as indicated by the galvanometer G establishes the condition

$$R_x + R_p = r_4 = \frac{r_1 r_3}{r_2} = \text{a constant}$$

where R_p is the internal resistance of the potentiometer between the galvanometer terminals, this usually being a variable depending upon the setting of the potentiometer. Making $r_3 = 9r_2$ we have $r_1 + r_2 = (r_1 + r_2 + r_3 + r_4)/10$ or $r_1 + r_2$ forms one-tenth of the resistance of the circuit, and accordingly the potential drop across these resistances, which is balanced against the emf of the thermocouple, equals one-tenth of the emf indicated by the setting of the potentiometer dials.

Stray emfs in the system are balanced out by setting the selective switch on the short-circuited segments *S*, switching battery b_2 to an

auxiliary resistance R' and adjusting circuit D until the galvanometer reading is unchanged by opening and closing the switch. Preferably the potentiometer should be set at approximately the correct reading in making this adjustment. The selective switch is then opened, battery b_2 is connected to the potentiometer, the galvanometer sensitivity is reduced by shunting with suitable resistances and the switch is connected to the desired couple. The potentiometer is adjusted to bring the galvanometer reading to zero and simultaneously the bridge is balanced to produce no change in reading upon closing the key. The latter adjustment should be more sensitive to changes in R_x than is the former.

If the bridge is balanced with circuit C closed through battery b_2, the battery current should be balanced against the standard cell with circuit B open, or what is the same thing, the battery may be switched to a suitable auxiliary resistance R' for standardizing. This method was employed in the present experiments.[8]

Two advantages of the use of resistance coils r_1 and r_2 in the present experiments are (1) that the resistance of circuit A is made much lower than could be obtained if R_p were included, this permitting the proper use of a galvanometer of low resistance, high sensitivity, and short period and (2) that such erractic stray emfs as might originate in the potentiometer are reduced by a factor of ten in the final measurements.

Fig. 3 shows the emf-temperature relation for the PtRh-Sn couple, the plotted data representing those of a single experiment. The tin forms the negative element of this couple and the alloy the positive element. By assigning negative values to the observed emf the chart corresponds to the usual thermoelectric diagrams. Over the limited temperature range here shown, the results may be represented by *two straight lines* intersecting at the melting point of tin. The *maximum*

[8] Similarly, if battery b_2 is balanced against the standard cell with circuit B closed, then B should be balanced with circuit C open, i.e. with b_2 connected to R'. An illustration of the advantageous use of this second method is the employment of a White potentiometer designed to give strictly constant resistance in the galvanometer circuit with the battery circuits open, in which case key K and battery b_1 could be eliminated. If the resistance of circuit C could be made simultaneously independent of the dial settings with circuit B closed, then manipulation would be reduced to the simplicity of the ordinary potentiometer. The method has its greatest applicability for the measurement of extremely small emfs, when the interaction of the above effects would become negligible and manipulation would be equally simple.

In adjusting circuit D to eliminate stray emfs, battery b_2 need not be replaced in circuit C by an equal resistance because of the negligible effect of leaving circuit C open during the operation.

deviation of any point from the straight lines is less than 0.1 microvolt. The difference in the slopes of the two lines gives for the thermoelectric power of solid tin versus liquid tin at the melting point,

$$\left(\frac{de}{dt}\right)_{\text{Liquid}} - \left(\frac{de}{dt}\right)_{\text{Solid}} = 1.2 \text{ microvolts / deg C}$$

where the liquid tin is at the higher potential.

Values found from similar experiments ranged from 1.0 to 1.6 microvolts / deg C, and our unpublished work of several years ago with iron-tin couples gave 1.4 microvolts / deg C. Probably the value $1.2 \pm .2$ microvolts / deg C represents a fair mean of our data.

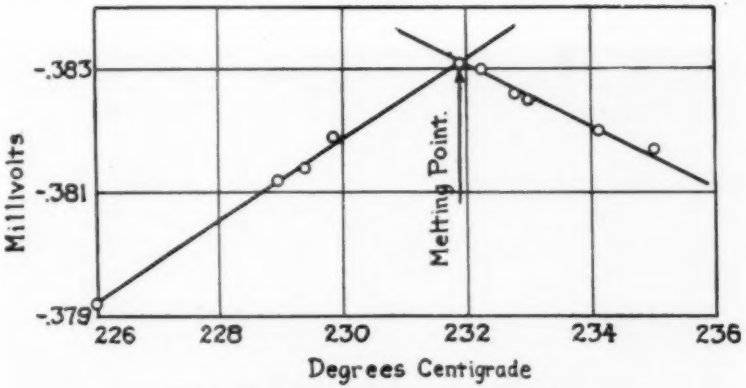

FIG. 3. *Emf-temperature diagram for PtRh vs Sn.*

Several experiments were performed in which a photographic recorder was employed to automatically draw the emf-temperature curve for the Sn-PtRh couple. While this method did not yield satisfactory numerical values because of the difficulty in calibrating the recorder, it is of interest in that it clearly demonstrated the existence of a *discontinuous* change in the thermoelectric power of tin at the melting point. The method is precisely that used in the Saladin recorder[9] except that galvanometers of higher sensitivity were employed. One galvanometer was connected to Couple B, Fig. 1, and the displacement of the moving mirror gives in the photographic chart a line of constant temperature. The other galvanometer was connected to couple A, so that displacement of the reflecting mirror of this instrument gives a line of constant emf at right angles to the line of constant temperature.

[9] Described by Burgess, "Measurement of High Temperatures" 3d ed, p. 419.

As the temperature t°C of the junction *D* is varied, the recorder automatically draws a calibration curve similar to that of Fig. 3.

Fig. 4 shows a typical record. The temperature in the region of the junction *D* of Fig. 1 was increased from about 215°C through the melting point of tin at 231.9° to about 245°C and was then allowed to fall, the calibration curve being traced in the order up *F* to *E*, down *B*, up *C* to *D*, back to *E* and down *A*. The galvanometer which was connected to couple *A* and produced the horizontal deflection had a longer period than the other galvanometer. Hence heating curves *F* and *B* are displaced to the left by amounts depending upon the rate of temperature rise at various points, while cooling curves *C* and *A*

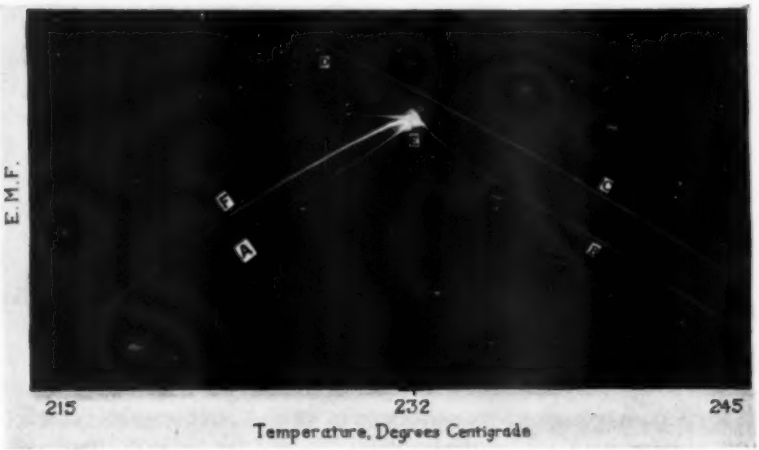

FIG. 4. *Autographic emf-temperature record for PtRh vs Sn.*

are similarly displaced to the right. The rate of temperature rise decreased as point *E* was approached along curve *F*, allowing the effect of the lag to decrease in this region. Curves *B* and *A* show how the lag was taken up after passing point *E*. Curve *C* shows no retardation in the cooling rate until suddenly the temperature and emf changed to condition shown by *E* more rapidly than could be followed by either galvanometer. Curvature of line *D* is caused by the difference in lags of the two galvanometers. The bright spot at *E* is halation occurring as the result of the arrest during freezing or melting. It will be noted that the tin undercooled without freezing about 4° and then rapidly changed to condition *E* when crystallization started.

This is more clearly illustrated by Fig. 5 in which the rates of heating and cooling were sufficiently slow that the lag of the galvanometers caused negligible displacement of the various branches, so that the heating and cooling curves coincided throughout.

We have in these two records, and in many similar ones not here reproduced, the proof of the existence of a thermocouple with one leg of solid tin and the other leg of supercooled liquid tin, the temperature of the hot junction being 231.9°C and that of the cold junction extending from this value to about 228°C. The emf developed by this anomalous couple is approximately 4.6 microvolts when the hot junction is at the melting point and the cold junction is at 228°C. The abrupt change in slope of the curves of Figs. 4 and 5 at the melting point of

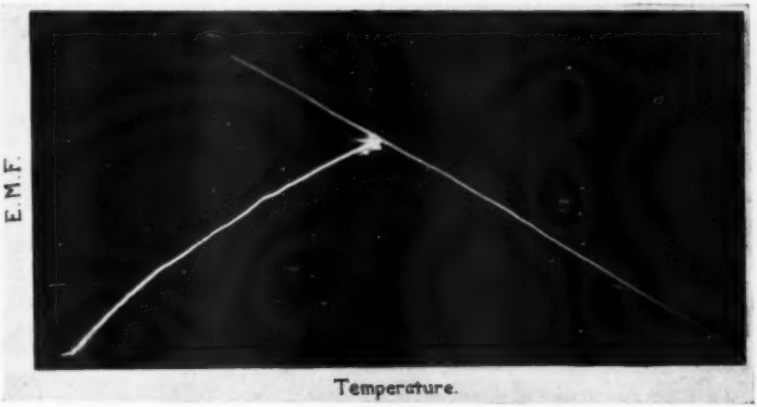

FIG. 5. *Autographic emf-temperature record for PtRh vs Sn.*

tin confirms the more precise experimental data given in Fig. 3. The discontinuous effect at the melting point has a real existence and can not be explained by a gradual transition in thermoelectric power over an extended temperature range.

The simple formula for thermoelectric power derived on the hypothesis of equilibrium between the current due to convection of electrons which are present in different concentrations and the current due to the compensating difference in potential is as follows:[10]

$$\frac{d}{d\theta}(e_L - e_S) = -\frac{R}{\epsilon} \ln \frac{N_S}{N_L}$$

[10] Richardson, The Electron Theory of Matter (1914), p. 461. It has been long recognized, as stated on page 462, that formulas of this type are very unsatisfactory.

when θ is the absolute temperature, R the gas constant reckoned for a single molecule, i.e. $1.37 \cdot 10^{-16}$ erg / °C, ϵ the electronic charge and N the number of free electrons per cm^3, the subscripts referring to the solid and liquid phases.

Northrup and Suydam[11] found that at the melting point the electrical conductivity of solid tin was 2.154 times as great as that of liquid tin. Since, by the simple electronic theory of conduction, conductivity is proportional to the number of free electrons we have $N_S / N_L = 2.154$. On substituting the values of the constants in the above equation we obtain:

$$\left(\frac{de}{d\theta}\right)_L - \left(\frac{de}{d\theta}\right)_S = -66 \text{ microvolts / deg C}$$

whereas the observed value is $+1.2$ microvolts / deg C. If the ratio N_S / N_L is deduced from a consideration of atomic volumes, the data show more satisfactory numerical agreement but the algebraic sign is again wrong, as has been pointed out by Koenigsberger.

If the Peltier emf is computed from the observed thermoelectric power we find

$$P = \left(\frac{de}{d\theta}\right)\theta = 0.6 \text{ millivolts}$$

between solid and liquid tin, the latter being at the higher potential. Since the simple electron theory requires that the metal having the higher conductivity, and hence the greater number of free electrons, be at the higher potential, we see that the theoretical value of the Peltier emf again has the opposite sign.

CHAMPION PORCELAIN CO.,
DETROIT, MICHIGAN,
BUREAU OF STANDARDS,
WASHINGTON, D. C.

[11] Northrup and Suydam J. Frank. Inst., *175*, p. 159; 1913.

THE DESIGN OF LARGE INCANDESCENT LAMPS

By P. G. Nutting

A number of problems connected with the design, rating, and use of very large incandescent lamps are of general interest to workers in related fields of illumination, pyrometry, and heat engineering. Interest naturally centers in the design formulas and in the high temperature data for tungsten.

An electric current flowing through a wire or ribbon imparts energy to it at a rate equal to the product of current and fall of potential, Ei. This will raise the temperature of the conductor until balanced by the escape of radiant energy from its surface.

(I) $$Ei = SA$$

S being specific radiation in watts / cm^2 corresponding to the stationary temperature attained and A being the area of the radiating surface. This equation is sufficient to determine either S or A, but is insufficient to determine the actual dimensions of the conductor. These may be determined if the specific resistance R of the material of the conductor at the temperature attained is known.

(II) $$E/i = Rl/c$$

in which l = length and c = cross section of the conductor. These two equations are sufficient to determine any two quantities in terms of the remaining four.

It may be noted that equations I and II contain three different sets of data, namely (1) the operating characteristics: voltage and current, (2) the thermal constants: radiation per unit area and specific resistance, and (3) the dimensions of the radiator. Their determination constitutes respectively the operating, rating, and the design problems, whether the radiator be intended for lighting or for heating.

In the design of any type of incandescent lamp, the matter of *life* to be attained and with it *temperature* of operation must first be decided. That life may be 1,000 hours for ordinary lighting, 50 hours for projection, or as low as 10 hours for lamps for special purposes, depending upon the relative importance of lamp costs. The dependence of life upon temperature varies somewhat with the form of filament whether straight or coiled, whether used in a vacuum or in a gas filled bulb. It can of course be determined only by experiment by burning a number

of lamps of each type. The temperature is roughly 2400°K for a life of 1,000 hours, 3,100 for a life of 100 hours, and 3,300°K for a life of 10 hours, but much depends upon selection of materials and care in construction.

Fundamental lamp data covering current, voltage, resistance, watts and candle power as functions of temperature were published by Langmuir in the January 1916, Physical Review. Subsequent work at the Nela Research Laboratory on the radiation from tungsten has developed improved data with a temperature scale based on the melting point 3650°K for tungsten as against 3520°K for Langmuir's data. An abstract of these data are given in the following table. Specific resistance is as reported by Forsythe and Worthing (Phys. Rev., p. 144; Aug., 1921) given by $R = KT^{1.20}$, $K = 6.255 \times 10^{-9}$. Specific Emission in watts / cm² is from recent unpublished data by Forsythe. Brightness in candles / cm² is from data published by Forsythe in the Physical Review, p. 436; April, 1922.

DATA ON HOT TUNGSTEN

Temperature T Degrees K (Nela)	Specific Resistance R	Specific Radiation S	RS	Brightness candles / cm²
2000	.0000572	23.8 (.26 BB)	.00136	20.1
2100	608	29.5	179	37.5
2200	640	36.8	236	61.7
2300	678	45.2	305	98.2
2400	710	56.2	400	155.5
2500	.0000750	68.6 (.31 BB)	.00515	232
2600	784	82.5	645	343
2700	821	98.0	805	483
2800	856	117.0	.01000	679
2900	894	136.0	.01220	910
3000	.0000930	158. (.34 BB)	.0147	1235
3100	968	182.	.0176	1600
3200	.0001005	211.	.0212	2105
3300	1043	242.	.0253	2660
3400	1081	276	.0300	3380
3500	.0001120	311. (.36 BB)	.0349	4220
3600	1160	355.	.0412	5200

The data of this table apply to *linear* filaments in a *vacuum*. Specific resistance R is of course independent of gas filling, coiling or crimping,

condition of the surface, emission of electrons, etc., but the apparent value of specific radiation S depends upon all of these. The formulas (I and II) are valid, but the value of S must be determined experimentally. It is to be noted that for fixed filament dimensions, the total watts is proportional to S, while the ratio of voltage to current (E / i) is independent of S. Further, on constant voltage, the product RS is invariant, therefore when R varies only moderately with temperature, it follows that both temperature and brightness are extremely sensitive to variations in surface emissivity.

The chief factors affecting energy consumed are the following:

1. Convection by the gas filling (about $\frac{1}{2}$ atmosphere cold, $1\frac{1}{2}$ hot, of nitrogen). This tends to increase energy consumption at a given temperature by an amount dependent not only upon gas pressure but size of bulb, form of radiator, room temperature, and filament temperature.

2. Coiling or crimping decreases the apparent value of S by decreasing the effective area freely radiating by an amount varying from practically nothing for hairpin filaments up to 40 or 50 per cent for closely coiled, closely spaced radiators.

3. Condition of Surface. The tabulated data relates to a surface prepared by drawing or rolling but without special treatment affecting its reflecting power. At a given temperature say $3000°K$, the emissivity of such a surface is only about 34 per cent that of a perfect radiator, but is much higher in the infrared than that of a highly polished surface. Its brightness is very nearly the same but much less energy is required to maintain a given temperature. More fundamental data on these three factors would be very useful in obviating cut-and-try methods.

As an illustration, consider a 30 kw lamp actually burning at $3200°K$ on 115 volts, 260 amperes. The filament is 2.8 mm in diameter and 270 cm long. Resistance = 0.44 ohm, specific resistance 0.0001005 ohms / cm^3. The radiator is formed into four coils side by side in series, covering an area 70×70 mm. Had the same lamp been made up in hairpin form in a vacuum it would have required 338 amperes at 148 volts (50 kw) to maintain the radiator at $3200°K$. In the coil form as made up, the consumption of energy and the radiation (and hence the effective value of S) is but 60 per cent of what each would be had the radiator been in linear form. Tungsten ribbon 4 mils (0.10 mm) thick having a surface like a mirror is available for lamp radiators. Only a few large lamps have yet been made up but observations on these indicate a net increase in efficiency of about 30 per cent.

In practice, the first step in the design of a new type of lamp is to determine the effective specific emission S for the form of filament required. This is done by determining E and i on a lamp (usually smaller) having a filament of known length and section, of the form desired, when operating at the required temperature. The value of S so determined is then used in computing the dimension of the radiation of the lamp to be designed. The calculations are exceedingly simple by the above formulas for either wire or ribbon filaments.

Many other details of design might be given but these are of little general interest. The production of both the 10 kw and 30 kw coiled wire radiator lamps are well through the development stage. Many difficult problems in construction peculiar to large lamps and high temperatures have been solved. A 100 kw lamp has been designed, but not yet constructed. Prior to a year ago a 3000 watt lamp was the largest ever in regular production.

SCHENECTADY,
NOVEMBER, 1922.

A PROJECTION AMMETER-VOLTMETER

By Howard M. Elsey

The usual type of large galvanometer used in demonstrating experiments in electricity or electro chemistry cannot be used in a large lecture room, particularly one where the scale must be viewed over a wide angle. For this reason, it was desired to obtain an instrument which could be used in connection with a projection lantern for demonstrating experiments in electro-chemistry.

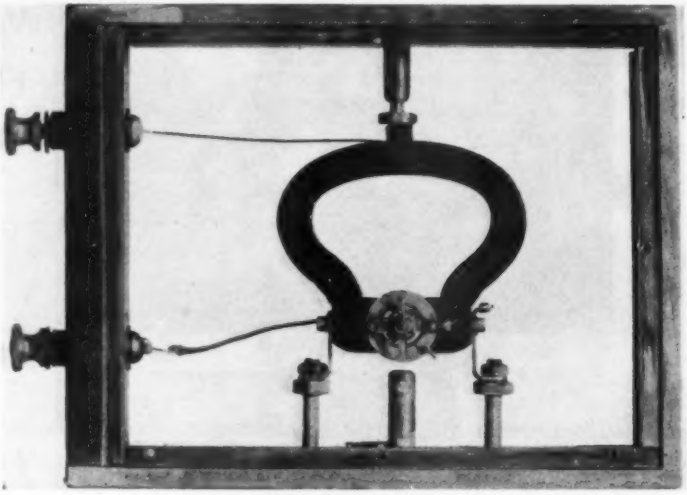

Fig. 1. *Projection ammeter-voltmeter with front, back and scale removed to show the placing of the moving system.*

Most of the ammeter or voltmeter moving systems are so large that they can not be placed in the slide carrier of a lantern. However, it was found that the moving system from a model 280, Miniature Precision Weston Meter was sufficiently small in its dimensions to be readily adapted to this use.

Fig. 1 shows the moving system mounted in a frame without the sides and scale. The frame is made of brass with the exception of one side which is of hard fiber and on which the binding posts are mounted.

All of the shunts and series resistances have been removed from the instrument. As it stands, it is simply a galvanometer which can be fitted with external shunts and resistances to convert it into an ammeter or voltmeter as desired.

Fig. 2 shows the completed instrument. The scale illustrated has been photographed on one of the glass windows. In the original

FIG. 2. *Completed projection ammeter-voltmeter.*

model 280 instrument, the scale lies immediately over the magnet of the instrument. For this reason, it was necessary to change the zero point of the instrument and the scale shown is purely an arbitrary one. It is believed that the instrument will be found useful in many laboratories.

DEPARTMENT OF CHEMISTRY,
UNIVERSITY OF KANSAS,
LAWRENCE, KANSAS,
FEBRUARY 8, 1923.

A METHOD OF INCREASING THE DISPERSION OF A CONSTANT DEVIATION SPECTROSCOPE*

By J. F. T. Young

During the course of some investigations of spectra in the visible region, it became a matter of some importance to increase the dispersion of a Hilger constant deviation glass spectroscope without

Increase in dispersion by addition of direct vision prisms to the Hilger constant deviation spectroscope.

Fig. 1. *Hg yellow lines.*
Fig. 2. *HHgg blue lines.*

losing the many advantages that this apparatus has in virtue of the fixed position of its collimator and telescope. This was successfully

*Communicated by Prof. J. C. McLennan.

done in a cheap and easy manner and it was thought that the method might be of use to others working in spectroscopy.

The principle was simply to insert one or more extra prisms between the telescope and the ordinary prism of the instrument and the whole solution of the difficulty was reached when direct vision trains were used in place of ordinary prisms. This arrangement worked very satisfactorily, the only possible drawback being that about 500 A. U. were cut off at each end of the range of the instrument. This, however, was overcome to a large extent by turning the original prism through a larger angle. The wave length drum of course lost its value to some extent in that it had to be recalibrated for visual observations, but if the work is being done by photography, as is usually the case, that is of no great importance.

Measurements taken of the dispersion in the region of the Hg yellow lines ($\lambda = 5790.87$ and $\lambda = 5769.81$) and the Hg blue lines ($\lambda = 4358.56$ and $\lambda = 4347.65$) gave the following results.

Region of Spectrum	Dispersion (A.U. per mm of the plate)		
	Normal Instrument	1 Direct Vision prism added	2 Direct Vision prisms added
Hg yellow.....	63	30	17
Hg blue.....	20	10	5

The increase in dispersion is well shown in the illustrations. Fig. 1 shows photographs of the Hg yellow lines under the conditions given in the Table above, and Fig. 2 those of the Hg blue lines. It will be understood, of course, that adding so much more glass to the optical system reduced the intensity considerably, but it was still quite good even with the largest dispersion.

UNIVERSITY OF TORONTO,
TORONTO, CANADA.